# Continuous 16.4-THz Bandwidth Coherent DWDM Transmission in O-band using a Single Fibre Amplifier System

**Daniel J. Elson[1,*], Vitaly Mikhailov[2], Jiawei Luo[2], Shohei Beppu[1], Glenn Baxter[3], Ralf Stolte[3], Luke Stewart[3], Shigehiro Takasaka[4], Mindaugas Jarmolovičius[5], Eric Sillekens[5], Robert I. Killey[5], Polina Bayvel[5], Noboru Yoshikane[1], Takehiro Tsuritani[1], and Yuta Wakayama[1]**

[1] *KDDI Research, Inc., 2-1-15 Ohara, Fujimino 356-8502, Japan*
[2] *OFS Laboratories, 19 Schoolhouse Rd., Somerset, New Jersey 08873, USA*
[3] *Finisar Australia, 21 Rosebery Ave, Rosebery, NSW 2018, Australia*
[4] *Furukawa Electric Co., Ltd., Ichihara 290-8555, Japan*
[5] *Optical Networks Group, UCL (University College London), UK*

[*] *xda-elson@kddi.com*

**Abstract:** A record transmission bandwidth of 16.4 THz is demonstrated in O-band using a single optical amplifier system. Performance is optimised by simultaneously mitigating inter-channel stimulated Raman scattering and nonlinear interference near the zero-dispersion frequency.


## 1. Introduction

Amidst the continuous surge in data traffic for artificial intelligence services, the bandwidth requirements especially for data centre interconnects (DCIs) have been experiencing a rapid increase [1–3]. To address these demands, ultrawideband transmission experiments have been reported utilising multiple bands [4–6]. The largest transmission bandwidth of 27 THz was demonstrated in E+S+C+L-band using five different types of fibre amplifiers, including distributed Raman, bismuth-, thulium-, and erbium-doped fibre amplifiers (E-band BDFAs, S-band TDFAs, C-band EDFAs, and L-band EDFAs). However, the throughput was limited by band (de)multiplexers and inter-channel stimulated Raman scattering (ISRS), especially at shorter wavelengths. To simplify the system, ultrawideband configurations using only a single type of amplifier without band (de)multiplexers have been proposed [7] with transmission bandwidth of 12.5 THz across S+C+L-band demonstrated using an ultrawideband semiconductor optical amplifier. A more attractive lower noise amplifier solution is O-band BDFAs with gain bandwidth in excess of 10 THz [8, 9]. A transmission bandwidth of 9.6 THz in O-band using a simple O-band BDFA was experimentally investigated [10]. Although the bandwidth was equivalent to the C+L-band, the O-band has further potential bandwidth up to 17.5 THz.

In this paper, we demonstrate a record transmission bandwidth of 16.4 THz using a single optical amplifier system. This was enabled by ultrawideband high-power BDFA, wavelength selective switch (WSS), and spectrally-shaped power optimisation, simultaneously mitigating nonlinear interference noise (NLIN) and ISRS across the O-band. The high-power BDFA exhibits more than 6-dB gain over a bandwidth of 17 THz and was used to boost the signal power transmitting over 80.4-km unrepeatered link. The ultrawideband WSS enabled us to shape the spectrum to mitigate both the ISRS power transfer and reduce the NLIN penalty near the zero dispersion frequency (ZDF). The power profile was optimised using the Gaussian Noise (GN) model [15]. To the best of our knowledge, this is the first investigation of the wideband transmission performance and its degradation due to the ISRS and NLIN around the ZDW.

## 2. Experimental Setup

Fig. 1 shows the experimental setup for the transmission system. This consisted of three test channels and amplified spontaneous emission (ASE) noise to fill 16.4 THz of bandwidth [11]. 327 × 48 GBd wavelength division multiplexed (WDM) signals on a 50 GHz grid, starting at 220.83 THz (1357.57 nm) and finishing at 237.13 THz

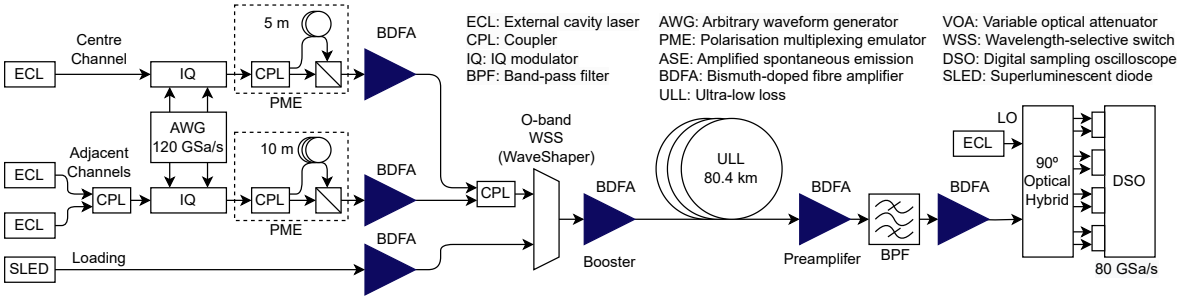


Fig. 1: Experimental setup for unrepeated transmission using BDFAs and WSS

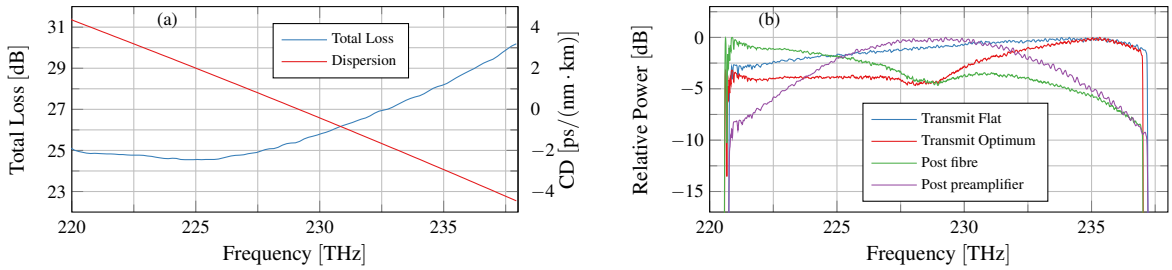


Fig. 2: Fibre characteristics (a) dispersion and loss profiles as a function of frequency for 80.4 km span (b) transmit and received spectra for both flat and optimised input power.

(1264.25 nm) were emulated using spectrally shaped ASE noise. The seed ASE noise source was a superluminescent diode (SLED) which was amplified with a BDFA. Each BDFA was single-stage with 250 metres of BDF, each pumped by a 915 nm uncooled laser diode via 915 to 1150 nm Yb-fibre based wavelength converter, with the design similar to that described in [13]. All amplifiers except the receiver pre-amplifier were counter pumped and had gain of >25.5 dB and typical noise figure of 5.5 dB for 0 dBm input power. The pre-amplifier was co-pumped and had 22.5 dB gain and 4.8 dB noise figure for 0 dBm input power. The flattening of the spectrum was performed by a COHERENT WaveShaper® 4000B which served as a wavelength-selective switch (WSS). This was used to control the input spectrum, add a notch for the test channels and combine with the channels under test. The input spectrum can be seen in Fig. 2. The three carrier lasers had a linewidth of <500 kHz and were modulated with different 16QAM payloads at 48 GBd in an odd-even configuration. To aid in decoding, quadrature phase shift keyed (QPSK) pilot symbols were inserted at a rate of 1/32 and a header of 1024 QPSK symbols was used for synchronisation [12]. Each IQ modulator was driven by an AWG at 128 GSa/s. Each set of channels was then polarisation multiplexed using a 3 dB coupler, delay lines of 5 and 10 metres (for odd and even, respectively) and recombined with a polarisation beam splitter. The central channel was used as the channel under test for all the measurements.

The transmission link was 80.4 km in length and made from AllWave® ULL single-mode optical fibre, compliant with ITU-T G.652.B. The measured total loss and dispersion profile is shown in Fig 2, where the ZDF was 228.90 THz (1309.71 nm). The low loss characteristics mean that the average loss for the span was 0.32 dB/km with a total loss of 24 and 30 dB at 220 and 238 THz, respectively.

After transmission, the signals were amplified with a BDFA and bandpass filtered with a width of 1.5 nm centred on the CUT. After filtering, the signal was amplified again to maintain power into the coherent receiver. The electrical signals were digitised at 80 GSa/s and processed offline. First, frequency offset removal was performed on only the pilot symbols before downsampling the entire frame to 2 samples per symbol for root-raised cosine filtering. Subsequently, a constant modulus algorithm was used to recover the distorted signal. The frame was downsampled to 1 sample per symbol for the carrier recovery, phase was estimated from the pilots and the correction was applied to the entire frame, finally, IQ orthogonalisation before calculation of bit error rate (BER), signal-to-noise ratio (SNR), generalised mutual information (GMI) and achievable information rate (AIR). AIR is calculated as the GMI minus the overhead from the inserted pilot symbols. No dedicated chromatic dispersion compensation step is performed.

## 3. Launch power optimisation

When transmission bandwidths are larger than 8 THz, ISRS can be significant. This shifts power from higher to lower frequencies (shorter to longer wavelengths) and can be seen effectively as an increase or reduction in apparent loss for higher frequencies and lower frequencies, respectively. The power tilt can be approximated as [14] $\Delta P = 4.3 \cdot P_{\text{tot}} C_r L_{\text{eff}} B$. where the attenuation $\alpha = 0.31$ dB/km, assumed Raman gain coefficient $C_r = 0.033$ 1/W · THz · km, $L = 80$ km, nonlinear effective length: $L_{\text{NL}} = (1 - \exp(-\alpha L))/\alpha = 14.4$ km, total launch power $P_{\text{tot}} = 26$ dBm and bandwidth $B = 16$ THz. The expected ISRS power transfer is up to 13.2 dB. The input and output spectrum was measured for various launch powers and is shown in Fig. 3a. When the total input power was within 10-16 dBm (-15 to -9 dBm/channel) the loss at low and high frequencies did not change, but after increasing the launch power over 16 dBm the power transfer is seen. At an input power of 21 dBm, the apparent loss at 238 THz increased by 2 dB and the apparent loss at 220 THz was reduced by 2 dB. The reduction in apparent loss subsequently occurred for every dB increase of launch power. By subtracting the loss of the fibre at the lowest input power where no ISRS is observed, the ISRS can quantified, as shown in Fig. 3b. The measured power tilt for an input power of 26 dBm was 13 dB.

To find the optimum launch power, both ISRS and NLIN near the ZDW must be taken into consideration. We use a fast ISRS integral GN model [15] considering the linear frequency dependence of the nonlinear coefficient $\gamma$ from 1.8 to 2.2 /W/km at 220 to 238 THz and of the effective area from 66.5 to 86.6 $\mu$m$^2$ at 228.8 to 193.4 THz. The total launch power was fixed to 23 dBm and 20 attenuation points across the bandwidth were optimised

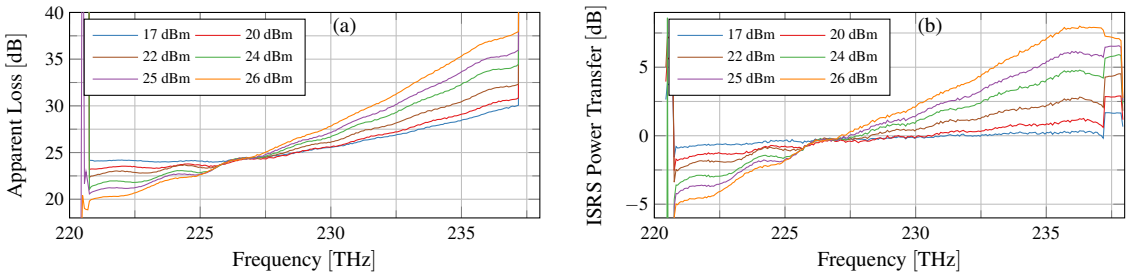


Fig. 3: (a) Apparent loss and (b) measured ISRS power transfer as a function of frequency for considered launch powers equivalent to −8 - +1 dBm/channel.

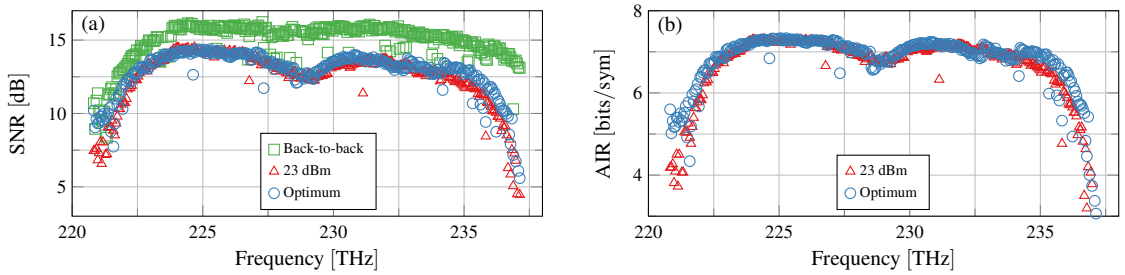


Fig. 4: (a) SNR and (b) achievable information rate measured over frequency.

for maximum capacity. Optimised input power for each channel was achieved by using the WSS iteratively to compensate for the nonlinear gain profile of the following BDFA.

## 4. Results and Discussion

Back-to-back characterisation of the transceiver was performed by removing the fibre span and replacing it with a 25 dB attenuation. The SNR of the central channel was measured as the three test channels and LO were swept from 220 to 238 THz. The results are shown in Fig. 4a. The highest achieved back-to-back SNR from a WDM channel was 16.5 dB at 230 THz, showing the need for further optimisation of the entire the transceiver chain.

The 80.4 km span was inserted, and the total launch was fixed to 23 dBm (-1.1 dBm/channel) and the input spectrum was set to flat. Afterwards, the SNR was measured as a function of frequency. The minimum SNR occurs at the highest frequency, for both launch powers where the combination of LO power, BDFA gain and fibre loss are all at the worst condition. In the centre of the transmission bandwidth, there is another drop in performance near the ZDF. The drop in performance is 2.4 dB compared to the best channel at 224 THz. The launch power is then adjusted to mitigate the effects of FWM and ISRS as shown in Fig. 2b. The loss in performance at ZDF is also mitigated down to 2 dB by the reduction in local launch power. The change in powers around this channel improved the SNR at the highest and lowest frequencies by 2 dB.

The measured AIR as a function of frequency is shown in Fig. 4b. The total potential throughput is taken as the sum of every channel's GMI multiplied by the symbol rate and subtracting the rate of pilot symbols. From these results, the maximum achievable throughput, assuming ideal FEC implementation, for the system with a flat input spectrum, was calculated to be 103.3 Tb/s and after optimisation improved to 106.0 Tb/s. This was an increase 0.5 bits/sym for the channels at the edges of the spectrum.

## 5. Conclusions

We have experimentally demonstrated ultra-wideband DWDM coherent transmission over a single span 80.4 km, using only one type of doped fibre amplifier. The launch power was optimised to simultaneously overcome the inter-channel stimulated Raman scattering and nonlinear noise near the zero dispersion frequency leading to a potential throughput of 106 Tb/s without any chromatic dispersion compensation. To the best of our knowledge, this work achieved the highest single amplifier transmission bandwidth, 16.4 THz, for an unrepeated single mode fibre link.

**Acknowledgements:** Support under UK EPSRC grants TRANSNET (EP/R035342/1), EWOC (EP/W015714/1) and EP/V007734/1 is gratefully acknowledged.

## References

1. M. Filer *et al.*, in J. Opt. Comm. Netw., **11**(10), (2019).
2. C. Xie, *et al.*, in Proceedings of the IEEE, **110**(11), 1699-1713, (2022).
3. D. Tauber *et al.*, J. Light. Technol., **42**(4), 1139–1151, (2023).
4. T. Kato *et al.*, Photon. Technol. Lett., **36**(1),16-19, (2023).
5. D. Soma *et al.*, *ECOC*, Th.C.2.2, (2023).
6. B. J. Puttnam *et al.*, *ECOC*, Th.C.2.4, (2023).
7. J. Renaudier *et al.*, *ECOC*, Th.PDP.A.3, (2017).
8. A. Khegai *et al.*, *OFC*, Tu1E.4, (2021).
9. Y. Wakayama *et al.*, J. Lightw. Technol. **41**(12) 3908-3915 (2023).
10. D. J. Elson *et al.*, J. Lightw. Technol., **42**(4), (2024)
11. D. J. Elson, *et al.*, Opt. Express **25**(16), 19529–19537 (2017).
12. Y. Wakayama, *et al.*, Opt. Express **29**(12), 18743-18759 (2021).
13. V. Mikhailov *et al.*, J. Lightw. Technol. **42**(4), 1265-1271 (2023)
14. D. Semrau, *et al.*, J. Lightw. Technol. **36**(14) 3046-3055 (2018).
15. M. Jarmolovičius, *et al.*, in arxiv.org 2401.18022 (2024).